

# Updated spherical harmonic moments of Ganymede from the Juno flyby

Tristan Weber<sup>1,2</sup>, Kimberly Moore<sup>3</sup>, John Connerney<sup>1</sup>, Jared Espley<sup>1</sup>, Gina  
DiBraccio<sup>1</sup>, Norberto Romanelli<sup>1,4</sup>

<sup>1</sup>NASA Goddard Space Flight Center, Greenbelt, MD, 20771, USA

<sup>2</sup>Howard University Department of Physics and Astronomy, Washington DC, 20059, USA

<sup>3</sup>California Institute of Technology, Division of Earth and Planetary Sciences, Pasadena, CA, 91125, USA

<sup>4</sup>Department of Astronomy, University of Maryland, College Park, MD, USA.

## Key Points:

- Using data from Juno's orbit 34 flyby of Ganymede, we present updated spherical harmonic moments of the moon's internal magnetic field.
- Ganymede's dipole moment is very dominant, with quadrupole moments that are over a factor of ten weaker than the main dipole term.
- No strong induction signature is expected during this flyby, allowing us to explore the relative importance of quadrupole terms.

---

Corresponding author: Tristan Weber, [tristan.weber@nasa.gov](mailto:tristan.weber@nasa.gov)

## Abstract

In this study, we use data from the Juno and Galileo spacecraft to analyze the internal magnetic dynamo of Ganymede. As the only known moon with a strong internal magnetic field, Ganymede is a uniquely interesting object in the context of understanding the formation and structure of planetary magnetospheres. Using a spherical harmonic model centered on the moon, we report a dipole approximation for Ganymede of  $g_0^1 = -716.4$  nT,  $g_1^1 = 56.0$  nT, and  $h_1^1 = 27.0$  nT. We find that using a quadrupole fit rather than a dipole fit provides only a marginal increase in accuracy, and instead favor the use of a dipole approximation until more data can be obtained. The magnetic moment estimates provided here can be used as a baseline for interpreting data from future spacecraft flybys of the moon, and can serve as inputs into numerical models studying Ganymede's magnetosphere.

## Plain Language Summary

Jupiter's moon Ganymede is the only known moon to possess its own strong internal magnetic field. This makes it a uniquely interesting planetary body in the context of understanding how planetary magnetic fields in the solar system form and interact with the space environment. Juno's recent flyby of the moon has provided us with a new set of spacecraft data from Ganymede for the first time in twenty years, and using that data we calculate a new best estimate of the properties of the moon's internal field. This estimate can be used as a baseline for future studies of Ganymede using data and numerical simulations.

## 1 Introduction

Ganymede is both the largest moon in our solar system and the only known moon to possess a global internal magnetic field, the discovery of which (M. Kivelson et al., 1996) spurred a variety of studies working to characterize the moon's unique properties. These works revealed that Ganymede, embedded in the corotating plasma of the Jovian magnetosphere, creates a magnetosphere that in many ways resembles a planetary magnetosphere in the solar wind. Ganymede's magnetic field dominates the local Jovian field, stands off the incoming plasma, and reconnects with the Jovian field to create open field lines that reach from the moon's poles out toward Jupiter (e.g. M. G. Kivelson et al., 1997; Williams et al., 1997). Particles precipitating along these open field lines create auroral emission (McGrath et al., 2013), while ionospheric particles flow outwards (Frank et al., 1997; Vasyliūnas & Eviatar, 2000), reminiscent of the polar outflows observed at Earth.

Unlike at other magnetospheres in the solar system, however, the plasma flowing past Ganymede is moving at subalfvenic, submagnetosonic speeds. With thermal and magnetic pressure dominating over ram pressure, this means that no bow shock is formed upstream of the moon, and that the magnetosphere takes a shape that more resembles a cylinder than it does the teardrop shape of familiar planetary magnetospheres. Due to this unique situation, Ganymede's magnetosphere has been the subject of many modeling studies. These have used a variety of different numerical schemes, including single-fluid MHD (Jia et al., 2009; Fatemi et al., 2016), multi-fluid MHD (Paty & Winglee, 2004, 2006), Hall-MHD (Dorelli et al., 2015), hybrid (Fatemi et al., 2016; Poppe et al., 2018; Romanelli et al., 2022), and particle-in-cell modeling (Tóth et al., 2016; Zhou et al., 2019).

Taken together, previous studies of Ganymede present an image of the moon that invites more attention: A magnetosphere featuring similar processes to those found in planetary magnetospheres, but in a plasma regime not found elsewhere in the solar system (Jia & Kivelson, 2021). As such, further investigations are forthcoming. With Juno's

recent flyby, we now have new data from Ganymede’s magnetosphere for the first time in twenty years, and the upcoming JUICE orbiter is expected to revolutionize our understanding of the moon.

For all of these investigations, it is crucial to have as accurate a representation as possible of the strength of the moon’s internal magnetic field. Our knowledge of the moon’s magnetic moments serves as a baseline for interpreting spacecraft data and as a fundamental input into numerical models. The most recent estimations of Ganymede’s internal dipole moment were provided by M. Kivelson et al. (2002), who used data from three of Galileo’s flybys of the moon to fit a spherical harmonic magnetic field model. With Juno’s recent flyby, we now have the opportunity to revisit this model and update the fit with more observations. In this study, we combine data from Galileo and Juno to estimate the internal magnetic moments of Ganymede. Following the method of M. Kivelson et al. (2002), we provide updated spherical harmonic coefficients for both a simple dipole fit and a quadrupole fit, and discuss the applicability of the quadrupole approximation.

In addition to possessing an internal magnetic field, Ganymede also may host a subsurface ocean of liquid water. Europa and Callisto are both known to have subsurface oceans, the first indications of which were the induced magnetic fields observed by Galileo (Khurana et al., 1998). Follow-up investigations searched for a similar inductive response at Ganymede, but the moon’s strong magnetic field made it difficult to observe smaller magnetic signatures of this kind (M. Kivelson et al., 2002). Specifically, studies of Ganymede’s magnetic field were unable to determine whether observed magnetic variations were due to an inductive response or to quadrupole terms in the moon’s internal field. A recent study using the Hubble space telescope analyzed time variations in Ganymede’s auroral ovals, and determined that the presence of subsurface ocean in the moon is likely (Saur et al., 2015), but in-situ signatures of magnetic induction have still never been observed. During Juno’s flyby of Ganymede, the moon was situated near the center of the Jovian magnetodisk, and as such we do not expect there to be a strong magnetic inductive signature present. This means, however, that our analysis of the flyby data is well-situated to examine more closely the relative importance of quadrupole terms in Ganymede’s field.

In section 2 of this paper, we present an overview of the flyby geometry and magnetic field data from Juno’s flyby of Ganymede. In section 3, we present our method of spherical harmonic analysis. In section 4, we present the results of our analysis and discuss our findings in relation to the previously calculated magnetic moments. And in section 5, we summarize our work and consider future implications.

## 2 Overview of Juno’s Ganymede flyby

### 2.1 Flyby geometry

An overview of Juno’s Ganymede flyby is shown in Figure 1. In this figure, the upper-right panel shows a time series of the measured vector magnetic field, while the other three panels show the flyby geometry in GphiO coordinates. In this Ganymede-centered coordinate system, +X points in the direction of Ganymede’s orbital motion, +Y points toward Jupiter, and +Z points in the direction of Jupiter’s spin axis. Because the Jovian plasma flow surrounding Ganymede moves more quickly than the moon’s orbital motion, +X GphiO also points in the direction of the wake, which is shown as a light gray shaded region in the flyby plots. To help interpret the three dimensional nature of the flyby geometry plots, one can visualize the lower-left panel as the front of a cube, and then picture folding the lower-right and upper-left panels inward onto two other faces of the cube.

Juno began the flyby in the positive X and negative Y quadrant, meaning that it was downstream from Ganymede on its anti-Jovian side. Over the course of the flyby,

Juno passed through the wake region, eventually ending slightly upstream from Ganymede on the moon's Jupiter-facing side. In panels a, c, and d, we have also plotted the trajectories of Galileo's G01, G02 and G28 flybys. These are the three crossings that were used by M. Kivelson et al. (2002) to model Ganymede's internal magnetic field, and will therefore be used in this study as well (the reasons for including these Galileo orbits while excluding others will be discussed later in the paper). From figure 1 we can see that Juno's flyby covers a different section of parameter space than the relevant Galileo orbits, particularly with regards to sampling the downstream wake region. This should prove helpful in our modeling of the moon's internal field, as increased coverage is beneficial in constraining multipole spherical harmonic moments.

## 2.2 Magnetic field measurements

The upper-right panel of Figure 1 shows magnetic field data from Juno's encounter with Ganymede. These measurements were taken by the Juno Magnetic Field investigation (MAG), which is composed of two sets of triaxial fluxgate magnetometers. MAG samples the vector magnetic field at a rate of 64 Hz and with a resolution of  $\sim 0.05$  nT (Connerney et al., 2017). During the flyby, Juno sampled several distinct regions of Ganymede's magnetosphere, signatures of which can clearly be seen in the magnetic field data. At 16:43, a field rotation is evident as Juno began to enter into the Ganymede system. Following this there is a period of increased variability in the magnetic field from 16:46 to 16:51 as Juno moved into Ganymede's wake region. Juno then moved to its closest approach of the moon, reaching an altitude of 1035 km at  $\sim 16:56$ . As expected, this corresponds to the strongest measured magnetic fields during the flyby, and after this point the magnetic field measurements become weaker until there is once again a field rotation at  $\sim 17:01$ , signaling Juno's exit from the Ganymede system.

In this study we also use data from the Galileo magnetometer, which used two triaxial fluxgate magnetometers to measure the vector magnetic field at a resolution of 3 Hz. We combine this data from Galileo with the measurements from Juno to fit a spherical harmonic model of Ganymede's internal field, as described in the next section.

## 3 Method of spherical harmonic analysis

### 3.1 Orbit Selection

Galileo performed eight flybys of Ganymede, but in our analysis we only use data from the G01, G02, and G28 flybys, as these were the orbits that M. Kivelson et al. (2002) used in their analysis of the moon's internal field. Other Galileo orbits were considered by that study, but were determined to be too far from the Moon to be useful in constraining quadrupole moments. See Figure 5 of that study for additional discussion of why other orbits were excluded, informed by a full analysis of the expected quadrupole contributions to the magnetic field measured by Galileo.

### 3.2 Background subtraction

The magnetic field measured during flybys by Juno and Galileo is a composition of both Ganymede's internal magnetic field and the background magnetic field of Jupiter. In order to accurately model Ganymede's internal dynamo, we therefore first need to remove the background Jovian field from our measurements. We accomplish this in the same manner as M. Kivelson et al. (2002), fitting a polynomial to the Jovian magnetic field measurements taken before and after the flyby. For each flyby, we fit a degree two polynomial to the magnetic field measurements taken before entering the ganymede system and after exiting it (as signaled by a large field rotation). We then subtract the result from our measurements to obtain data representing just Ganymede's internal magnetic field.

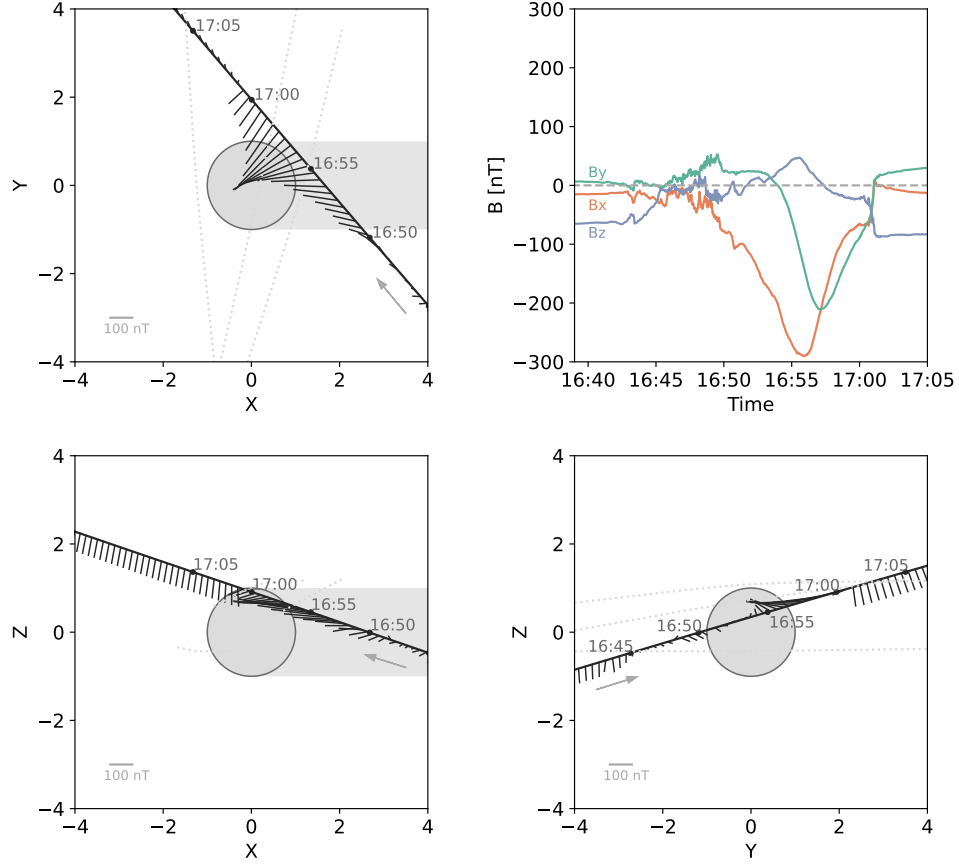


**Figure 1.** Magnetic field measurements from the Juno flyby of Ganymede. The upper-right panel shows a time-series of the data, while the other three panels show Juno's trajectory through the Ganymede system. The thinner lines anchored in Juno's trajectory represent the measured vector magnetic field averaged over every thirty seconds, and the shaded gray region represents Ganymede's wake. All of the panels in this figure use the GphiO coordinate system, which is defined in the text.

### 3.3 Method of least-squares fitting

After removing the background magnetic field for each orbit, we then combine the data from Galileo and Juno and perform a least-squares fit across all of the orbits at once. Because the Juno magnetometer takes data at a higher time resolution than Galileo, the Juno flyby contains a much higher total number of measurements. This means that the Juno flyby will be weighted much more highly by the fitting analysis if no modifications are made. We would prefer that each flyby is weighted equally, as gaining information from several parts of the spatial parameter space is vital for spherical harmonic analysis. We therefore downsample the Juno measurements to be at the same cadence as Galileo.

Similarly, a standard least-squares fitting routine will by default weight the fit most strongly toward the measurements with the highest field magnitude, meaning that the fit will be optimized primarily for the flybys that passed closest to the moon and measured the strongest fields. To counteract this, we follow the method of M. Kivelson et al. (2002), applying a weighting method where the data from orbit  $i$  is weighted inversely by  $B_{max}^i / (\sum_i (B_{max}^i)^2)^{1/2}$ , with  $B_{max}^i$  representing the largest field magnitude measured during that orbit.

We fit the data to a model consisting of a multipole moment centered at Ganymede and a uniform cartesian background magnetic field (we denote this background field as UFX, UFY, UFZ, using GphiO coordinates). The uniform background fields are intended to approximate magnetopause currents, and are allowed to vary from orbit to orbit, while the multipole moment is not allowed to vary between the passes. We perform the fit for both a dipole field and a quadrupole field. In the dipole case, we are fitting three spherical harmonic coefficients ( $g_0^1, g_1^1, h_1^1$ ) along with four different sets of three parameters that represent the uniform fields during each flyby. This gives us a total of 15 parameters. In the quadrupole case, we once again have four sets of three parameters representing the uniform fields, but are now fitting eight spherical harmonic coefficients ( $g_0^1, g_1^1, h_1^1, g_2^0, g_2^1, g_2^2, h_2^1, h_2^2$ ), giving us a total of 20 parameters. A full description of our least-squares fitting method is provided in Appendix A.

## 4 Results and Discussion

The results of our analysis are shown in Table 1. We present the magnetic moments obtained from both the dipole and quadrupole fits, along with the corresponding uniform fields found for each orbit. The performance of the fit for each orbit is plotted in Figure 2, where the spacecraft measurements are shown with solid lines and the model fits with dotted lines.

Our addition of Juno's flyby does not drastically change the multipole fits found by M. Kivelson et al. (2002). Using just the Galileo orbits, that study reported a  $g_0^1$  term of -727.3 nT when fitting a dipole with uniform background fields. We find that the addition of Juno data changes this  $g_0^1$  term to -716.4 nT. The secondary dipole moments for this fit are comparably small for both studies (a few tens of nT). In fitting a quadrupole, we find a slightly larger change, with M. Kivelson et al. (2002) reporting a  $g_0^1$  term of -711.0 nT while we find a  $g_0^1$  of -748.3 nT. However, the quadrupole fit only represents a minor increase in performance when compared to the dipole fit. Our dipole fit had an RMS value of 10.0 nT, and the quadrupole fit an RMS of 8.3 nT. We would naturally expect the fit to become more accurate when adding in five extra parameters, but the accuracy increase here is quite minor. Furthermore, we find the quadrupole terms ( $g_2^0$  through  $h_2^2$ ) to be smaller than the  $g_0^1$  term by more than an order of magnitude, suggesting that the main dipole field of Ganymede is very dominant. For these reasons, we conclude that the use of a quadrupole fit is in danger of overfitting the data, and is not justified here. We suggest that the dipole fit should be treated as the most accurate representation we have until more data is obtained, and that deviations from the dipole field

could still be the result of small quadrupole terms or induction from a subsurface ocean, as suggested by M. Kivelson et al. (2002)

The question of whether induction from a subsurface ocean is present at Ganymede was investigated by M. Kivelson et al. (2002), but was left as an open question to the future. That study favored a subsurface ocean as the explanation for magnetic field variations observed between orbital passes, but the authors did not view their evidence conclusive enough to treat the subject as fully closed. Unfortunately, the Juno flyby of Ganymede occurred when the moon was found close to the center of the magnetodisk, when any induction signature that is present is expected to be at its weakest point. For this reason, we were unable to use Juno data to provide further analysis of induction signatures, and we leave that question to future studies with expanded datasets.

	$g_0^1$	$g_1^1$	$h_1^1$	$g_2^0$	$g_2^1$	$g_2^2$	$h_2^1$	$h_2^2$	UFX	UFY	UFZ	RMS
<b>Dipole Fit</b>	-716.4	56.0	27.0	-	-	-	-	-				10.0
									<b>G01</b>	31.7	3.2	-36.5
									<b>G02</b>	38.1	99.9	28.6
									<b>G28</b>	-1.4	-42.9	76.3
									<b>Juno</b>	-7.0	57.8	-25.9
<b>Quadrupole Fit</b>	-748.3	41.1	20.8	22.5	23.3	-26.8	16.5	-10.6				8.3
									<b>G01</b>	30.9	1.5	-32.7
									<b>G02</b>	37.7	84.9	24.0
									<b>G28</b>	-9.4	-52.0	48.7
									<b>Juno</b>	-8.2	58.5	-22.8

**Table 1.** Magnetic moments resulting from spherical harmonic fits using Juno and Galileo data. The dipole and quadrupole moments are fixed for all passes in the fit, while the uniform background fields are allowed to vary from orbit to orbit. UFX, UFY, and UFZ represent uniform, cartesian background fields in the GphiO coordinate system. RMS is the root-mean-square calculated over all of the orbits for the corresponding fit. All entries are in units of nanotesla.

## 5 Summary

In this study we used data from the Galileo and Juno spacecraft to fit a spherical harmonic model to the internal magnetic field of Ganymede. The magnetic moments resulting from this analysis are presented in Table 1. We found that the addition of data from Juno only slightly changed the previous reported results from Galileo, and that the main dipole field is greater than the other multipole moments by over an order of magnitude. We favor the use of a dipole approximation, as the quadrupole fit does not perform substantially better and is still dominated by the main dipole term.

The upcoming JUICE mission, scheduled to launch in April of 2023, will be the first spacecraft ever to orbit Ganymede (or any moon other than Earth's). One of JUICE's primary mission objectives is to study Ganymede's intrinsic magnetic field and its interactions with the Jovian magnetosphere, and over the several years that JUICE is expected to orbit the moon it will provide us with a wealth of data to accomplish that objective. The work presented in this study may serve as a baseline of comparison for the studies that JUICE will enable.

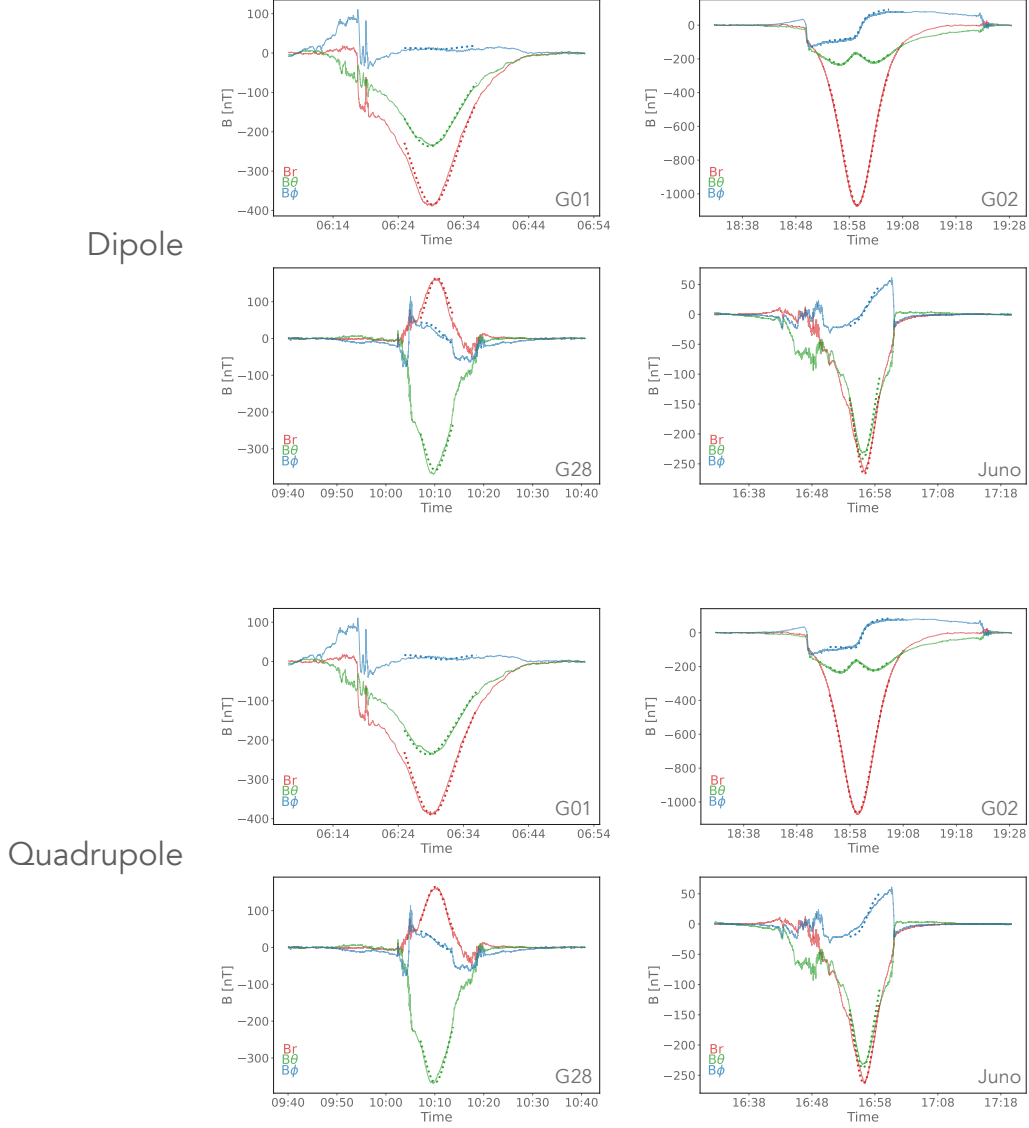


**Figure 2.** Data-model comparison for spherical harmonic fits using Juno and Galileo data. In each panel, the measured magnetic field for that orbit is shown with solid lines, while the dotted lines represent the field calculated from the magnetic moments shown in Table 1. These panels all use the Gsph coordinate system, a Ganymede-centric, spherical system in which  $r$  is the radial distance,  $\theta$  is the colatitude measured from the rotation axis, and  $\phi$  is the longitude as measured from the Jupiter-facing meridian. The top set of 4 panels fit a dipole to the data, while the bottom set of four fit a quadrupole.



## Appendix A Least Squares Fitting

In this study we use a weighted least-squares fit, combining data from multiple flybys to find a single set of multipole components, while allowing constant background components to vary for each flyby. This amounts to solving the matrix equation  $\mathbf{b} = \mathbf{A}\mathbf{x}$ , where  $\mathbf{b}$  is the measured magnetic field data,  $\mathbf{x}$  is the matrix of coefficients that we wish to solve for, and  $\mathbf{A}$  is the matrix relating these two as a function of spacecraft position. To find where the square of the error ( $\mathbf{A}\mathbf{x} - \mathbf{b}$ ) is minimized, we solve the equation

$$\frac{d}{d\mathbf{x}} \frac{1}{2} (\mathbf{A}\mathbf{x} - \mathbf{b})^T (\mathbf{A}\mathbf{x} - \mathbf{b}) = 0 \quad (\text{A1})$$

which reduces to

$$\mathbf{x} = (\mathbf{A}^T \mathbf{A})^{-1} \mathbf{A}^T \mathbf{b} \quad (\text{A2})$$

Because a least square fit biases toward fitting the data with the highest magnitude, our fit is by default optimized for the flybys with the strongest magnetic fields and lowest orbital altitudes. In order to weight our separate flybys more equally, we use the same method as M. Kivelson et al. (2002) and weight the data from each orbit inversely by  $B_{max}/(\sum_i (B_{max})^2)^{1/2}$ , with  $B_{max}$  representing the largest field magnitude measured during that orbit. Modifying equation A2 to include this weighting method, we have

$$\mathbf{x} = (\mathbf{W}\mathbf{A}^T \mathbf{W}\mathbf{A})^{-1} \mathbf{W}\mathbf{A}^T \mathbf{W}\mathbf{b} \quad (\text{A3})$$

For each data point in  $\mathbf{b}$ , we have three components of the magnetic field as measured in the Gsph coordinate system. The matrix  $\mathbf{A}$  corresponding to that measurement takes the form  $[\mathbf{A}_{sph}, \mathbf{UF}_{G1}, \mathbf{UF}_{G2}, \mathbf{UF}_{G28}, \mathbf{UF}_{Juno}]$ . Here,  $\mathbf{A}_{sph}$  represents the submatrix of schmidt-normalized coefficients from the spherical harmonic expansion, which depends only on spacecraft position (see e.g. Connerney, 1981; Connerney et al., 2018, for a full description of these terms). For a dipole fit, this submatrix will be size  $3 \times 3$ , while for a quadrupole fit it will be  $3 \times 8$ . The  $\mathbf{UF}$  submatrices relate the cartesian background fields for each orbit to the Gsph coordinate system. Because the data from each orbit only affects one of these submatrices, for any given data point the three  $\mathbf{UF}$  submatrices that don't correspond to that orbit will be 0, while the  $\mathbf{UF}$  matrix corresponding to that orbit takes the form

$$\begin{pmatrix} \sin(\theta) \cos(\phi) & \sin(\theta) \sin(\phi) & \cos(\theta) \\ \cos(\theta) \cos(\phi) & \cos(\theta) \sin(\phi) & -\sin(\theta) \\ \sin(\phi) & \cos(\phi) & 0 \end{pmatrix} \quad (\text{A4})$$

## Acknowledgments

This material is based upon work supported by NASA under award number 80GSFC21M0002. KMM is supported by the 51 Pegasi b Fellowship through the Heising-Simons Foundation. All data used in this study can be found on the planetary plasma interactions on the planetary data system. The Galileo data can be found at <https://tinyurl.com/GanymedeData>. The Juno data can be found at <https://tinyurl.com/JunoGanymedeData>.

## References

Connerney, J. (1981). The magnetic field of jupiter: A generalized inverse approach. *Journal of Geophysical Research: Space Physics*, 86(A9), 7679–7693.

- Connerney, J., Benn, M., Bjarno, J., Denver, T., Espley, J., Jorgensen, J., ... others (2017). The juno magnetic field investigation. *Space Science Reviews*, 213(1), 39–138.
- Connerney, J., Kotsiaros, S., Oliverson, R., Espley, J., Joergensen, J. L., Joergensen, P., ... others (2018). A new model of jupiter’s magnetic field from juno’s first nine orbits. *Geophysical Research Letters*, 45(6), 2590–2596.
- Dorelli, J. C., Gloer, A., Collinson, G., & Tóth, G. (2015). The role of the hall effect in the global structure and dynamics of planetary magnetospheres: Ganymede as a case study. *Journal of Geophysical Research: Space Physics*, 120(7), 5377–5392.
- Fatemi, S., Poppe, A., Khurana, K., Holmström, M., & Delory, G. (2016). On the formation of ganymede’s surface brightness asymmetries: Kinetic simulations of ganymede’s magnetosphere. *Geophysical Research Letters*, 43(10), 4745–4754.
- Frank, L., Paterson, W., Ackerson, K., & Bolton, S. (1997). Outflow of hydrogen ions from ganymede. *Geophysical research letters*, 24(17), 2151–2154.
- Jia, X., & Kivelson, M. G. (2021). The magnetosphere of ganymede. *Magnetospheres in the Solar System*, 557–573.
- Jia, X., Walker, R. J., Kivelson, M. G., Khurana, K. K., & Linker, J. A. (2009). Properties of ganymede’s magnetosphere inferred from improved three-dimensional mhd simulations. *Journal of Geophysical Research: Space Physics*, 114(A9).
- Khurana, K., Kivelson, M., Stevenson, D., Schubert, G., Russell, C., Walker, R., & Polanskey, C. (1998). Induced magnetic fields as evidence for subsurface oceans in europa and callisto. *Nature*, 395(6704), 777–780.
- Kivelson, M., Khurana, K., Russell, C., Walker, R., Warnecke, J., Coroniti, F., ... Schubert, G. (1996). Discovery of ganymede’s magnetic field by the galileo spacecraft. *Nature*, 384(6609), 537–541.
- Kivelson, M., Khurana, K., & Volwerk, M. (2002). The permanent and inductive magnetic moments of ganymede. *Icarus*, 157(2), 507–522.
- Kivelson, M. G., Khurana, K., Coroniti, F., Joy, S., Russell, C., Walker, R., ... Polanskey, C. (1997). The magnetic field and magnetosphere of ganymede. *Geophysical Research Letters*, 24(17), 2155–2158.
- McGrath, M. A., Jia, X., Retherford, K., Feldman, P. D., Strobel, D. F., & Saur, J. (2013). Aurora on ganymede. *Journal of Geophysical Research: Space Physics*, 118(5), 2043–2054.
- Paty, C., & Winglee, R. (2004). Multi-fluid simulations of ganymede’s magnetosphere. *Geophysical research letters*, 31(24).
- Paty, C., & Winglee, R. (2006). The role of ion cyclotron motion at ganymede: Magnetic field morphology and magnetospheric dynamics. *Geophysical research letters*, 33(10).
- Poppe, A., Fatemi, S., & Khurana, K. (2018). Thermal and energetic ion dynamics in ganymede’s magnetosphere. *Journal of Geophysical Research: Space Physics*, 123(6), 4614–4637.
- Romanelli, N., Dibaccio, G., Modolo, R., Connerney, J., Ebert, R., Martos, Y., ... Bolton, S. (2022). Juno magnetometer observations at ganymede: comparisons with a global hybrid simulation and indications of magnetopause reconnection. *Geophysical Research Letters*.
- Saur, J., Duling, S., Roth, L., Jia, X., Strobel, D. F., Feldman, P. D., ... others (2015). The search for a subsurface ocean in ganymede with hubble space telescope observations of its auroral ovals. *Journal of Geophysical Research: Space Physics*, 120(3), 1715–1737.
- Tóth, G., Jia, X., Markidis, S., Peng, I. B., Chen, Y., Daldorff, L. K., ... others (2016). Extended magnetohydrodynamics with embedded particle-in-cell simulation of ganymede’s magnetosphere. *Journal of Geophysical Research: Space*

- 327 *Physics*, 121(2), 1273–1293.
- 328 Vasyliūnas, V. M., & Eviatar, A. (2000). Outflow of ions from ganymede: A reinter-  
 329 pretation. *Geophysical research letters*, 27(9), 1347–1349.
- 330 Williams, D., Mauk, B., & McEntire, R. (1997). Trapped electrons in ganymede’s  
 331 magnetic field. *Geophysical research letters*, 24(23), 2953–2956.
- 332 Zhou, H., Tóth, G., Jia, X., Chen, Y., & Markidis, S. (2019). Embedded kinetic sim-  
 333 ulation of ganymede’s magnetosphere: Improvements and inferences. *Journal*  
 334 *of Geophysical Research: Space Physics*, 124(7), 5441–5460.